Physics and Astronomy, School of Physical and Chemical Sciences,
University of Canterbury, Christchurch, New Zealand

Modelling Molecular Clouds with Potential Cosmic Ray Accelerators

Rhia Hewett - 63153776

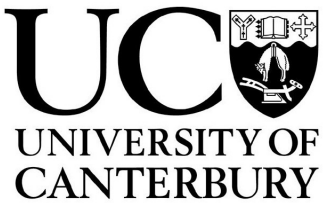

PHYS391 Project 2023

Supervisors: Prof. Jenni Adams,

Dr. Sabrina Einecke*, and Ryan Burley*

*from the University of Adelaide, Australia

Abstract

The search for cosmic ray accelerators in our galaxy capable of producing protons of PeV energies is ongoing. While currently the best candidates are supernova remnants (Hillas, 2005), cosmic rays from these sources cannot be observed directly so instead, to verify this hypothesis, we look to detect neutral messengers: gamma rays and neutrinos. In this study, a python pipeline was produced to model the interaction of molecular clouds, which provide a dense target material for neutrino production, with supernova remnants as cosmic ray accelerators. The neutrino flux for each of 176 candidate pairs was predicted and the top 5 pairs with the highest observable neutrino flux were ranked. The top combination was found to be the SNR G332.4-00.4 with the molecular cloud at (333.46, -0.31). This was also selected as one of the brightest gamma ray targets by Mitchell et al. (2021), demonstrating the viability of this model.

Contents

Chapter 1

Introduction

The research produced from neutrino detectors, like the IceCube Neutrino Observatory in Antarctica, has established the importance of multi-messenger astronomy in the study of high energy astrophysics. One of the key areas of research that neutrino detection contributes to is the study of high energy cosmic ray acceleration (Pandya & Seckel, 2019). The mechanism for acceleration of cosmic rays up to PeV energies within our galaxy is not well understood and cannot be confirmed with direct observation of cosmic rays from their source. Detection of neutrinos produced in the particle interactions of cosmic rays offers an alternative means for studying and verifying potential cosmic ray accelerators as demonstrated by IceCube Collaboration (2016). This study seeks to produce a viable python model for such neutrino production from the interaction of cosmic ray accelerators with nearby molecular clouds.

1.1 Cosmic Ray Energy Spectrum

Cosmic rays are ionised nuclei, like protons, accelerated to high energies from galactic and extragalactic bodies.

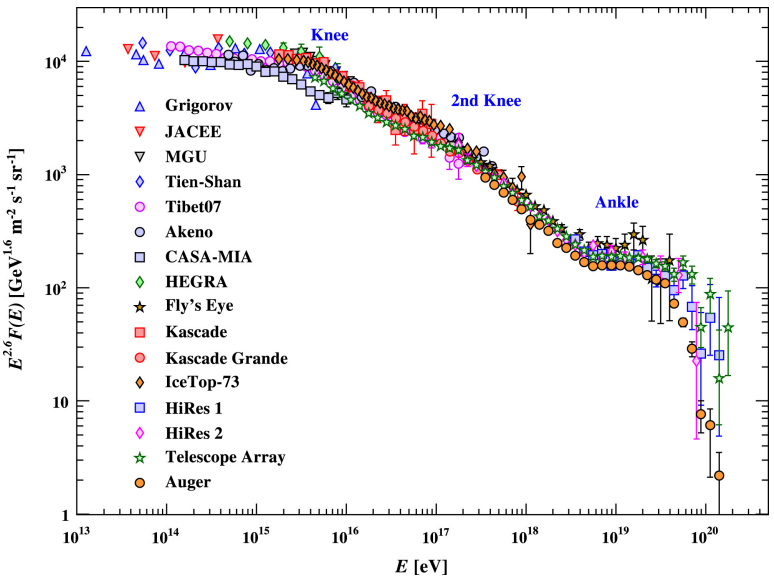

Figure 1.1: Cosmic ray energy spectrum, as observed by various detectors, from Mollerach & Roulet (2018)

The energy spectrum for cosmic rays, as observable to us on Earth, is defined by a power law relationship from GeV to EeV energies. At the PeV region of the energy spectrum some unusual features emerge as illustrated in Figure 1.1 by Mollerach & Roulet (2018). This has become the focus of much high energy cosmic ray research. These features include most notably a drop of the spectrum at about 3 PeV, called the 'knee'. This is often explained as the transition between galactic and extra-galactic sources (Gaisser et al., 2013).

This study investigates potential cosmic rays accelerators within our galaxy that can reach up to the PeV cutoff of the knee feature, to verify the viability of the transition hypothesis for the 'knee' feature.

1.2 Supernova Remnants as Cosmic Ray Accelerators

Supernova remnants (SNRs) are frequently proposed as the main candidates for sources of galactic cosmic rays. The mechanism for acceleration in SNRs is a diffuse shock front produced from supernova ejecta. Collisions with the dense, high velocity gas of the SNR shock front due to moving magnetic inhomogeneities, both upstream and downstream, can cause repeated acceleration until the cosmic ray particle escapes into the interstellar medium (Hillas, 1984). This process is termed the 1st order Fermi acceleration mechanism and it is the best theory currently posited to explain the order of energy gain needed to match observation as discussed by Bell (2013). Acceleration of this nature is most likely to occur during the Taylor-Sedov phase of SNR evolution. where adiabatic expansion takes place (Celli et al., 2019).

There is also a significant restriction placed on the acceleration capacity of an SNR by the geometry of the system. Thus maximum acceleration energy will be met when the binding potential of the magnetic field within the SNR shockfront is exceeded. A cosmic ray with a Larmor radius of $R_L = mv_\perp/qB$ can only be confined within a system of a greater radius - this is often termed the Hillas criterion (Hillas, 1984). For SNRs, this typically limits the energy of accelerated cosmic rays to the PeV range. This makes supernova remnants good candidates for cosmic ray accelerators within our galaxy that could reach the PeV 'knee' cutoff.

1.3 Cosmic Ray Detection

Cosmic rays carry a charge and are therefore deflected from magnetic fields within the galactic plane. Because of this, their direction of origin cannot be resolved and traced back to their source.

Neutrinos are neutral messengers produced as a result of cosmic ray interaction with a medium. Cosmic ray protons will collide with particles in the medium, producing pions and muons in the process, as in Equation 1.1.

$$p + p \longrightarrow \pi_\pm \quad \text{or} \quad p + p \longrightarrow \pi_0 \tag{1.1}$$

$$\pi_\pm \longrightarrow e_\pm + \nu_e(\bar{\nu_e}) + \nu_\mu(\bar{\nu_\mu}) \quad \text{or} \quad \pi_\pm \longrightarrow \mu_\pm + \nu_\mu(\bar{\nu_\mu}) \tag{1.2}$$

$$\pi_0 \longrightarrow \gamma\gamma \tag{1.3}$$

The pions and muons will go on to decay into electron and muon neutrinos as in Equation 1.2, which can then be detected and their directionality resolved to point back to the source of the interactions. In this study, only the muon neutrino contribution is investigated but the electron neutrino contribution can be inferred from the 2:1 flavour ratio in the reaction scheme (Ahlers et al., 2016). It must be noted here that the observable neutrino flux will not necessarily come from the cosmic ray source itself, but the location of proton-proton interactions.

Molecular clouds of hydrogen gas provide dense target material for these interactions and therefore should point to nearby SNRs with an observable neutrino flux, as posed by Gabici & Aharonian (2007).

The aim of this study was to produce a python model that predicts the neutrino flux produced in molecular clouds in close proximity to SNRs as potential cosmic ray accelerators. From this, a list of the top candidate combinations as been produced to help inform likely targets for neutrino detectors. In the event of an observed neutrino flux from these targets, the hypothesis of SNRs as the PeV comic ray accelerator in our galaxy would be strengthened.

Chapter 2

Candidate Selection

Candidate SNR and molecular cloud combinations were selected from the catalogues discussed below, with a few additional selection criteria. The data available from these catalogues provided the input parameters for the python model.

2.1 SNR Candidates - SNRcat

The catalogue used to produce SNR candidates is SNRcat by Ferrand & Safi-Harb (2012). This is an online live catalogue compiled from the latest SNR observations. In this study, the data from the catalogue was taken as of December 2022. For each of the 383 SNR candidates, the catalogue includes the position in galactic coordinates, upper and lower age estimates (in yr) from which an average was calculated, and upper and lower distance estimates (in kpc). It must be noted that the distance estimates often feature a wide range of uncertainty. As such, in this study the distance estimates are not used directly but instead are used to restrict SNR candidates to those in close proximity to a molecular cloud. SNR candidates were removed if they fell outside of the Taylor-Sedov age range (1500-50000 yr) as suggested by Mitchell et al. (2021)

2.2 Molecular Cloud Candidates - Green's Catalogue

The molecular cloud catalogue used was Rice et al. (2016). This was complied from the galactic CO survey by Dame et al. (2001) for a total of 1063 candidates. For each molecular cloud candidate, the catalogue provides galactic coordinates, radius (in pc), mass (in solar masses) and distance estimates (in kpc). The distance estimates were verified by Rice et al. (2016) via the observed size-linewidth relation for molecular clouds and using an assumed constant scale height. For this reason, the distance values for combinations are taken to be that of the cloud.

The particle number density for each cloud was also calculated from the radius (r) and mass (M) estimates. This was done via Equation 2.1 assuming spherical symmetry and uniform density for the cloud, where $\mu_1 = 1.36$ as the mean mass per particle in the gas of the cloud and $m_H = 1.66 \times 10^{-27}$ kg for the mass per hydrogen atom.

$$n = \frac{M}{\frac{4}{3}\pi\mu_1 m_H r^3} \tag{2.1}$$

2.3 Candidates Combinations

Candidate combinations are selected as SNR and cloud pairs that lie within 100pc of each other. Due to the large uncertainty range of the SNR distance estimates, determining the separation distance is difficult. First, combination where the SNR has a distance range that does not fall within 1 kpc of the distance of a given cloud are removed. Then the separation distance is calculated as a projection of the angular separation between SNR and cloud with respect to the cloud distance. This produced 176 candidate combinations.

Chapter 3

Outline of Python Pipeline

The python pipeline developed in this study predicts the neutrino flux produced in molecular clouds in close proximity to SNRs, as a function of neutrino energy. This consists of establishing the proton spectrum injected from the SNR, where the protons then diffuse through the interstellar medium (ISM) to interact, producing neutrinos when they reach the molecular cloud. This approach primarily follows the methods implemented in Mitchell et al. (2021).

In the development of this model, two versions were produced: a simple model of diffusion in the ISM from which a second time dependant model was built to include the evolution of the SNR shockfront and energy dependent release of protons. Both models share the same overall structure. Cosmic ray production from the SNR is represented as power-law proton injection spectrum of order $\alpha = 2$. A probability distribution function (PDF), designed to account for diffusion in the ISM, is then applied. This defines a proton density according to the given PDF ($f(E, R, t)$) as a function of energy (E_p in eV), for a distance (R' in cm) from the SNR shockfront at a time (t' in s) since the protons were released, as in Equation 3.1 below from Aharonian & Atoyan (1996).

$$J_p = N_0 \cdot E_p^{\alpha} \cdot f(E, R, t) \tag{3.1}$$

The normalisation constant (N_0) is given in Equation 3.2, determined by the energy available from the supernova explosion for acceleration of cosmic ray protons (E_{CR}), along with the maximum and minimum of the proton energy range (E_{max} and E_{min}). The cosmic ray energy budget E_{CR} is set to 10^{50} ergs for a canonical supernova, as suggested by Aharonian & Atoyan (1996).

$$N_0 = E_{CR}/(\ln E_{max} - \ln E_{min}) \tag{3.2}$$

The proton density is evaluated at the centre of the cloud to generate a resultant muon neutrino flux from the interaction cross section and energy probability spectrum for neutrino production via pion decay in proton-proton collisions. The integral for the neutrino flux as a function of neutrino energy (E_ν) is given in Equation 3.3.

$$\phi_\nu(E_\nu, R', t') = cn \int_{E_\nu}^{\infty} \sigma_{inel}(E_p) J_p(E_p, R', t') F_\nu(\frac{E_\nu}{E_p}, E_p) \frac{dE_p}{E_p} \tag{3.3}$$

Here, $\sigma_{pp}(E_p)$ is the interaction cross section for proton-proton collisions, defined in Equation 3.4 as in Kafexhiu et al. (2014). The number density (n in cm^{-3}) is that of the molecular cloud and c is the speed of light.

$$\sigma_{pp}(E_p) = (30.7 - 0.97\log(\frac{E_p}{E_{thres}}) + 0.18\log^2(\frac{E_p}{E_{thres}}) \times (1 - (\frac{E_{thres}}{E_p})^{1.9})^3 \tag{3.4}$$

$F_\nu(x, E_p)$ is the neutrino energy spectrum that represents the probability of neutrino production from pion decay which is given in detail in Appendix A.

The neutrino flux integral is generated using a trapezium numerical method from the scipy.integrate python package. It involves an internal proton energy spectrum from the given neutrino energy (E_ν) up to a maximum proton energy of 1 PeV as restricted by the Hillas Criterion for SNR cosmic ray accelerators.

When the neutrino flux is evaluated at a selected energy, a predicted flux observable on Earth can be produced using Equation 3.5. In this simplified model, the neutrino flux at the centre of the cloud is treated as an average for the cloud as a whole. Here, d is the distance from the cloud to Earth.

$$F(E_\nu) = \frac{\frac{4}{3}\pi r^3 \phi_\nu(E_\nu)}{4\pi d^2} \tag{3.5}$$

3.1 PDF Model 1 - Simple ISM Diffusion

The first version of the probability distribution function follows the work of Aharonian & Atoyan (1996). It is a simple model of proton diffusion during travel through the ISM from SNR to molecular cloud, as illustrated in Figure 3.1. All protons are released at the beginning of the supernova, from its centre. They then diffuse through the ISM to the cloud centre, where neutrinos are produced.

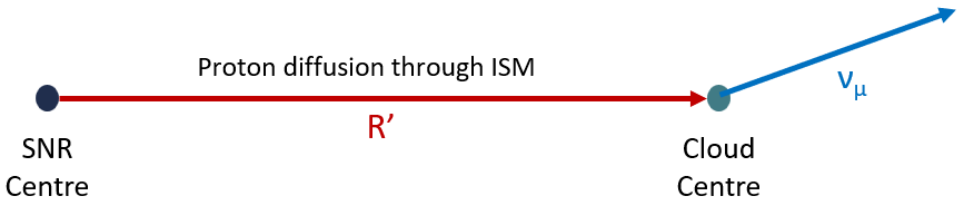

Figure 3.1: Schematic of the first PDF model, with proton diffusion in the ISM.

The PDF for this model is given in Equation 3.6 below, where t' is the SNR age (in s) and R' is the distance from the SNR centre to the molecular cloud centre (in cm).

$$f(E_p, R', t') = \frac{1}{\pi^{3/2} R_d^3} \exp(-\frac{(\alpha - 1)t'}{\tau_{pp}} - \frac{R'^2}{R_d}) \tag{3.6}$$

The proton interaction time (τ_{pp} in years) is approximated as $\tau_{pp} = 6 \times 10^7/n$ (yr) as suggested by Aharonian & Atoyan (1996). The number density of the ISM (n_0) is 1cm^{-3}.

A diffusion radius (R_d in cm) is established according to Equation 3.7 which is an approximation valid for diffusion within the ISM when ($\tau_{pp} << t'$) as discussed in Mitchell et al. (2021).

$$R_d = 2\sqrt{D(E)t'} \tag{3.7}$$

$D(E)$ (in $\mathrm{cm^2 s^{-1}}$) is a diffusion factor given in Equation 3.8 as in Mitchell et al. (2021), with a power-law dependence on energy of order $\delta = 0.5$.

$$D(E) = \chi D_0 (\frac{E/GeV}{B/3\mu G})^{\delta} \tag{3.8}$$

Here, χ is a suppression coefficient for diffusion within molecular clouds and B is the magnetic field strength within the medium. However, proton penetration within the molecular cloud is not yet considered in this study, so χ is set to 1 and B is set to a constant $3\mu G$ for diffusion in the ISM, with values suggested by Mitchell et al. (2021). D_0 is a diffusion coefficient, which is set for slow diffusion with $D_0 = 3 \times 10^{26}$ from Mitchell et al. (2021).

3.2 PDF Model 2 - Shockfront Evolution

The final version of the model produced in this study follows much of the methods previously established, but with a few notable improvements produced with reference to Mitchell et al. (2021). The overall result is a more complex representation of proton release from the SNR, with a time dependent shockfront and an energy dependent time of release, as in Figure 3.2.

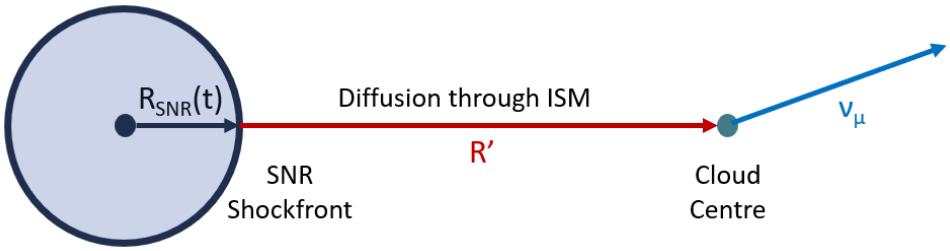

Figure 3.2: Schematic of the final PDF model, with evolving SNR shockfront.

Two additional components are implemented to achieve this. The first is a prediction of the shockfront radius (R_{SNR} in pc) for an SNR at a given time (t in yr) since the supernova occurred, as given in Equation 3.9. For this, the number density of the ISM (n_0) is $1\mathrm{cm^{-3}}$, and a factor of 1.4 is applied as the mean mass per particle (μ_1).

$$R_{SNR}(t) = 0.31(\frac{(E_{SN}/10^{51}erg)}{(n_0/cm^{-3})(\mu_1/1.4)})^{1/5}(t/yr)^{2/5} \tag{3.9}$$

The second is a prediction of the escape time for a given proton with energy (E_p in eV) as given in Equation 3.10.

$$t_{esc}(E) = t_{Sed}(\frac{E_p}{E_{Max}})^{-1/\beta} \tag{3.10}$$

These expressions, developed in detail by Celli et al. (2019), are applicable to SNRs undergoing adiabatic expansion in the Taylor-Sedov phase. They suggest parameter β is best estimated as 2.5 for middle-aged SNRs. The Sedov time (t_{Sed}) corresponds to the time at which the Taylor-Sedov phase begins. For a core collapse supernova with ejecta of 10 solar masses, this is approximately 1600 years, according to Mitchell et al. (2021).

This allows for a more accurate prediction of proton travel through the ISM. The time spent in the ISM for a proton of a given energy is then $t' = t_{SNR} - t_{esc}$. The distance travelled in the ISM is $R' = R - R_{esc}$, where R_{esc} is the SNR radius evaluated at t_{esc}: $R_{esc} = R_{SNR}(t_{esc})$. This becomes the time and distance input for the PDF.

The PDF itself was also improved with methods from Mitchell et al. (2021). The PDF for the second model is given in Equation 3.11. A normalisation factor is introduced to account for the release of protons from an evolving shockfront radius, as stated in Equation 3.12.

$$f(E_p, R', t') = \frac{f_0}{\pi^{3/2} R_d^3} \exp(-\frac{(\alpha - 1)t'}{\tau_{pp}} - \frac{R'^2}{R_d}) \tag{3.11}$$

$$f_0 = \frac{\sqrt{\pi} R_d^3}{(\sqrt{pi} R_d^2 + 2\sqrt{\pi} R_{SNR}^2) R_d + 4 R_{SNR} R_d^2} \tag{3.12}$$

The proton interaction time (τ_{pp}) is also updated in Equation 3.13, now defined by the inelastic cross section for proton-proton interactions ($\sigma_{pp}(E_p)$) as a function of proton energy. Here, the interaction inelasticity (κ) is set to 0.45.

$$\tau_{pp} = \frac{1}{n_0 c \kappa \sigma_{pp}(E_p)} \tag{3.13}$$

Chapter 4

Results and Analysis

For each candidate combination, the parameters recorded in the SNR and modlecular cloud catalogues were applied to produce proton density and neutrino flux spectrums at the centre of the cloud, according to Equation 3.1 and Equation 3.3 respectively with a selected PDF.

Plots of the proton density and neutrino flux output for each PDF model is presented below. The proton density spectra are shown in Figure 4.1 and the neutrino flux spectra in Figure 4.2. The PDF model 1 on the left is compared to the PDF model 2 on the right.

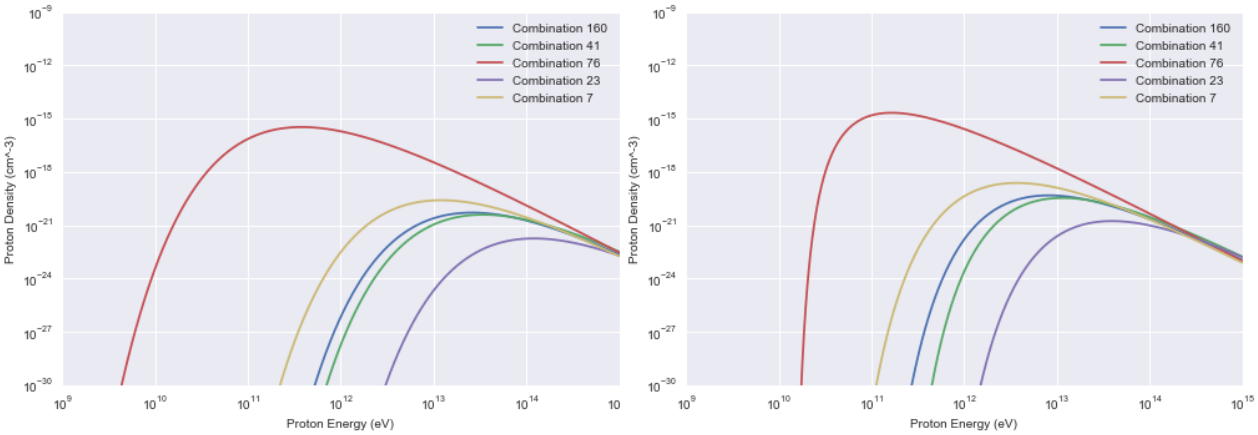

Figure 4.1: Proton density spectrum evaluated at the centre of the cloud as a function of proton energy, for PDF 1 on the left and PDF 2 on the right, featuring the top 5 candidate combinations.

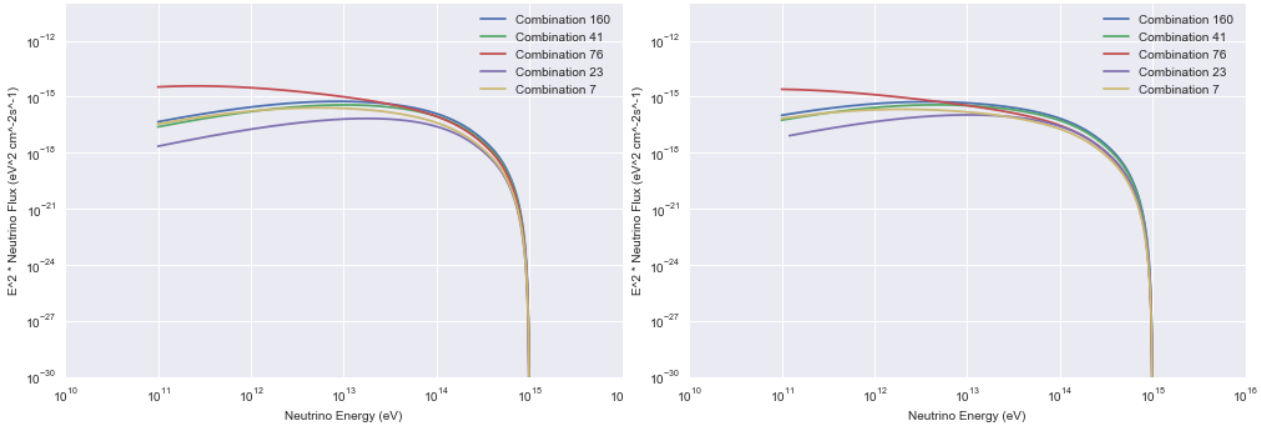

Figure 4.2: Neutrino flux spectrum produced at the centre of the cloud as a function of neutrino energy, for PDF 1 on the left and PDF 2 on the right, featuring the top 5 candidate combinations.

The second PDF model was selected for use in all further analysis. A predicted observable flux for each candidate combination was calculated via Equation 3.5 for neutrino energies of 1 TeV and 100 TeV. Candidates were ranked according to their observable neutrino flux at 100 TeV. The top 5 candidate combinations are presented in this study. These are listed along with their predicted observable neutrino flux at 1 TeV and 100 TeV in Table 4.1

Combo Index	SNR Name	Cloud Position (l, b) (deg)	F ($\mathrm{cm^{-2}s^{-1}TeV^{-1}}$) $E_\nu = 1$ TeV	$E_\nu = 100$ TeV
160	G332.4-00.4	(333.46, -0.31)	1.93e-12	3.16e-17
41	G035.6-00.4	(34.99, -0.96)	1.45e-12	3.00e-17
76	G107.5-01.5	(110.43, 1.89)	9.46e-12	2.15e-17
23	G029.7-00.3	(28.77, -0.09)	3.13e-13	1.80e-17
7	G018.9-01.1	(16.97, 0.53)	1.52e-12	1.43e-17

Table 4.1: Top 5 candidate combinations ranked by predicted neutrino flux at 100 TeV, as modelled via PDF 2.

Chapter 5

Discussion

The top candidate combination with the highest predicted neutrino flux at 100 TeV as observed on Earth was found to be the SNR G332.4-00.4 with the molecular cloud at (333.46, -0.31). The study done in Mitchell et al. (2021), where instead the gamma ray flux was modelled, also predicts this combination in their top 4 ranking of the brightest molecular clouds in a slow diffusion regime. This can be seen as a good confirmation of the viability of the python model produced in this study.

The shape of the proton density and neutrino flux output was also verified in personal communication with Ryan Burley and Sabrina Einecke at the University of Adelaide, Australia, who are working on a model similar to that implemented in Mitchell et al. (2021).

However, it should be noted that an few inconsistencies have been identified. The most significant is that the neutrino flux output at 100 TeV is much lower than that reported in correspondence with the University of Adelaide. The top combination here has a flux of $3.16 \times 10^{17}\text{cm}^{-2}\text{s}^{-1}\text{TeV}^{-1}$ while the reported fluxes are of order 10^{-13}. The neutrino flux aligns much better with this scale in the 1 TeV range, where the top combination has a flux of $1.93 \times 10^{12}\text{cm}^{-2}\text{s}^{-1}\text{TeV}^{-1}$. A similar discrepancy was found in the proton density output, namely that the proton spectrum begins at energies lower than expected for a selected combination (combo 41).

These problems have currently been attributed to an improvement in diffusion length function implemented in the model of Mitchell et al. (2021). Their model accounts for diffusion within the cloud while the model in this study models diffusion in the ISM only. It is likely that this simplification allows protons of a lower energy that should diffuse away in the cloud medium to instead reach the cloud centre, while the higher energy protons leave too quickly. Another possible explanation is that the energy dependant proton escape time has not been implemented correctly. More work is needed here to confirm the exact cause of each discrepancy and resolve them.

There were some assumptions made to simplify the production of the python model that may limit its representation of molecular cloud interaction with SNR cosmic ray accelerators. Firstly, the molecular clouds are treated as spherically symmetric with a uniform density. This unlikely to be an accurate representation of the cloud geometry, and future models could attempt to map and implement any observed irregularities in observations of the clouds. This model also does not account for the contributions of multiple SNR to the same molecular cloud. Some cases of this have been investigated by Mitchell et al.(2021), which would be of interest if these clouds were used as targets for neutrino detectors.

Chapter 6

Conclusion

This investigation was conducted to produce a python model that predicts the neutrino flux emitted from molecular clouds in close proximity to potential SNR cosmic ray accelerators. This was done to suggest likely targets for neutrino detectors in search for confirmation of SNRs as galactic PeV accelerators. The final model predicts a list of the top 5 candidates with the highest predicted observable neutrino flux. The top candidate was the SNR G332.4-00.4 with the molecular cloud at (333.46, -0.31) which is listed in the top 4 gamma ray sources reported by Mitchell et al. (2021). While a few discrepancies were found, the model has proven to be viable with respect to previous work.

Acknowledgements

I would like to thank my supervisor Jenni Adams for the advice and guidance she has given me over the summer. I would also like to thank Ryan Burley and Sabrina Einecke from the University of Adelaide, Australia, for their correspondence and suggestions regarding the production of the python model and verification of results.

References

Mollerach, S., & Roulet, E. (2018). *Progress in high-energy cosmic ray physics.* Progress in Particle and Nuclear Physics, 98, 85–118. https://doi.org/10.1016/j.ppnp.2017.10.002

Aharonian, F. & Atoyan, A. (1996). *On the emissiyity of π_0-decay gamma radiation in the vicinity of accelerators of galactic cosmic rays.* Astronomy and Astrophysics. 309. 917-928.

Bell, A. R. (2013). Cosmic Ray Acceleration. Astroparticle Physics, 43, 56–70. https://doi.org/10.

Hillas, A. M. (1984). *The origin of ultra-high-energy cosmic rays. Annual Review of Astronomy and Astrophysics*, 22(1), 425–444. https://doi.org/10.1146/annurev.aa.22.090184.002233

Hillas, A. M. (2005). *Can diffusive shock acceleration in supernova remnants account for high-energy galactic cosmic rays? Journal of Physics G: Nuclear and Particle Physics*, 31(5). https://doi.org/10.1088/0954-3899/31/5/r02

Kelner, S. R., Aharonian, F. A., & Bugayov, V. V. (2006). *Energy spectra of gamma rays, electrons, and neutrinos produced at Proton-proton interactions in the very high energy regime.* Physical Review D, 74(3). https://doi.org/10.1103/physrevd.74.034018

Mitchell, A. M., Rowell, G. P., Celli, S., & Einecke, S. (2021). *Using interstellar clouds to search for Galactic PeVatrons: Gamma-ray signatures from supernova remnants.* Monthly Notices of the Royal Astronomical Society, 503(3), 3522–3539. https://doi.org/10.1093/mnras/stab66

Ahlers, M., Bai, Y., Barger, V., &; Lu, R. (2016). Galactic neutrinos in the TEV to pev range. Physical Review D, 93(1). https://doi.org/10.1103/physrevd.93.013009

Pandya, H., & Seckel, D. (2019). *Search for PeV Gamma Rays and Astrophysical Neutrinos with IceTop and IceCube* (PhD dissertation). University of Delaware.

Kappes, A. for the IceCube Collaboration (2016). Exploring the universe with very high energy neutrinos. Nuclear and Particle Physics Proceedings, 273-275, 125–134. https://doi.org/10.101

Rice, T. S., Goodman, A. A., Bergin, E. A., Beaumont, C., & Dame, T. M. (2016). *A uniform catalog of molecular clouds in the milky way.* The Astrophysical Journal, 822(1), 52. https://doi.org/10.3847/0004-637x/822/1/52

Ferrand, G., & Safi-Harb, S. (2012). *A census of high-energy observations of Galactic Supernova Remnants.* Advances in Space Research, 49(9), 1313–1319. https://doi.org/10.1016/j.asr.201

Appendix A

Energy Spectrum of Neutrinos

The neutrino energy spectrum $F_\nu(x, E_p)$ gives the probability of neutrino production in proton-proton collisions as developed in detail by Kelner (2006). There are two contributions: the first from pion decay as in Equation A.1 and the second from muon decay as in Equation A.5. These components are then added together: $F_\nu(x, E_p) = F_\nu^{(1)} + F_\nu^{(2)}$. In these equations, $L = \log(E_p/TeV)$ and $y = x/0.427$.

$$F_\nu^{(1)} = B' \frac{\ln(y)}{y} \left(\frac{1 - y^{\beta'}}{1 + k' y^{\beta'} (1 - y^{\beta'})}\right)^4 \times \left(\frac{1}{\ln(y)} - \frac{4\beta' y^{\beta'}}{1 - y^{\beta'}} - \frac{4k'\beta' y^{\beta'} (1 - 2y^{\beta'})}{1 + k' y^{\beta'} (1 - y^{\beta'})}\right) \tag{A.1}$$

...where parameters B', β' and k' are given in Equations A2-4.

$$B' = 1.75 + 0.204L + 0.010L^2 \tag{A.2}$$

$$\beta'' = 1/(1.67 + 0.111L + 0.0038L^2) \tag{A.3}$$

$$k'' = 1.07 - 0.086L + 0.002L^2 \tag{A.4}$$

$$F_\nu^{(2)} = B'' \frac{(1 + k''(\ln(x))^2)^3}{x(1 + \frac{0.3}{x^{\beta''}})} (-\ln(x))^5 \tag{A.5}$$

...where parameters B", β'' and k" are given in Equations A6-8.

$$B'' = 1/(69.5 + 2.65L + 0.3L^2) \tag{A.6}$$

$$\beta'' = 1/(0.201 + 0.062L + 0.00042L^2)^{1/4} \tag{A.7}$$

$$k'' = \frac{0.279 + 0.141L + 0.0172L^2)}{0.3 + (2.3 + L)^2} \tag{A.8}$$